COMPARATIVE STUDY OF FLAME BEHAVIOR IN INDUSTRIAL KILN SYSTEMS

Adnan Ghareeb Tuaamah Al-Hasnawi[1, 2], Eckehard Specht[1]

[1]*Institute of Fluid Dynamic and Thermodynamic, Otto von Guericke University*
University Square 2, Magdeburg
39106, Germany, adnan_tuaamah@yahoo.com (A.A.)
[2]*Electromechanical Engineering, University of Technology*
Baghdad, Tal Muhammad, Baghdad
10066, Iraq, eckehard.specht@ovgu.de (E.S.)

Received 13 November 2025
Accepted 14 April 2026
DOI: 10.59957/jctm.v61.i4.2026.15

ABSTRACT

Annular ring burners are widely used in industrial kilns, such as tunnel, shaft, and rotary kilns, because they provide consistent and controlled burning. To investigate how operational parameters, such as air to fuel ratio, air velocity, O_2 concentration in combustion gases, and air inlet diameter, affect flame behaviour, including temperature distribution and flame length, this study uses ANSYS Fluent to simulate non - premixed methane flames in a rotary kiln. The results show that lower intake diameters are associated with increased air velocity, which leads to shorter flames. Additionally, compared to flames in combustion gas conditions, flames in ambient air have higher peak temperatures and longer durations.

Keywords: computational fluid dynamics, combustion, non - premixed flame, annular ring burners.

INTRODUCTION

In modern industry, the rotary kiln is widely used. Also, it is used in many situations such as the cement industry and metallurgy. To improve the temperature of the materials, burners are the essential part of rotary kilns. The operation and efficiency of the furnace are greatly affected by the performance of the burners [1]. Based on different features, for example, the type of fuel and the way of combustion chamber (down-firing, up-firing, side-firing burners), burners have also different classifications [2, 3]. According to the air supply system, burners can be divided into natural draught burner and forced draught burner. According to the kind of fuel, burners can be divided into gas, liquid and combined burners [2, 4]. In this paper, the annular ring burner with gaseous fuel is used, and this is a kind of gas burner. In addition, the air injected from the burner will be given an initial velocity, so it is a forced draught burner. Fuel and air are blended inside the furnace by non-premixed cylindrical or annular ring burners. They have higher volumes and lower temperatures than premixed flames, which lowers the danger of NO_x and flashback but may result in instability and blow-off [5]. Incomplete reactions, refractory damage, and temperature fluctuations can result from flame instability [6]. Burner shape, fuel type, and flow rate all influence flame behaviour, which in turn affects kiln efficiency and maintenance expenses [7]. To assess the Steady Diffusion Flamelet and EDC models, a 2D axisymmetric CFD simulation examined mixing and combustion in a radiant tube burner utilizing CO, OH, and temperature. In comparison to 3D simulations, 2D findings were deemed adequate for testing the FGM model [8]. Experiments and 3D CFD using the κ - ε for turbulence model and S2S model for heat transfer were used to study the heating of big, forged blocks in a gas-fired furnace. The furnace temperature fluctuated up to 200 K after loading, with temperature differences between simulation and experiment of about 7 %. The study showed promise for big steel part heat treatment optimization [9]. Flamelet combustion and

κ - ε turbulence models were used in the computational design of an annular combustion chamber for a CFM - 56 engine utilizing HEXPRESS and NUMECA. Complete combustion, little CO and NO emissions, and the absence of unburned hydrocarbons were observed in methane fuel at axial, 45°, and 60° injection angles [10]. A novel injector is used in a new continuous kiln design to move hot air from the cooling to the firing zone. The temperature distribution was examined using a 3D ANSYS Fluent model that took cone length, burner streamlining, and air volume into account. A 90 m s^{-1} air velocity at the burner cone facing the main flow produced the ideal temperature [11]. The experimental and numerical results of high-pressure rocket combustion were compared using OH emission imaging. The pseudo-OH pictures produced by radiative transfer equations in two CFD models shown good agreement between data for both laminar and turbulent fires, 3D CFD simulations, and 2D tests [12]. With deep learning providing real-time monitoring for effective production, refuse-derived fuel (RDF) in cement kilns provides a sustainable solution by lowering greenhouse gas emissions, preserving resources, and promoting the circular economy. Furthermore, compared to 3D simulations, 2D axisymmetric CFD simulations of a radial tube burner employing different combustion models showed adequate accuracy, confirming their application in the investigation of premixed combustion [13]. Using air preheating, ammonia and methane were burned in a self-recuperative annular tube porous burner, demonstrating increased flame stability and efficiency, nevertheless, NO emissions still need to be adjusted [14]. Furthermore, a rotary kiln's 3D ANSYS simulations showed that boosting secondary air flow lowers emissions and increases combustion efficiency [15]. The increasing interest in hydrogen utilization has raised safety concerns related to its transport and combustion behaviour. Numerical simulations have shown that hydrogen concentrations below 22 % are insufficient to mitigate hazardous thermal radiation. As a result, the transportation of hydrogen - natural gas blends through existing pipeline infrastructure poses a risk of dangerous jet flames in the event of leakage. In these studies, the non-premixed chemical equilibrium combustion model provided the closest agreement with experimental data [16]. Accurate validation of combustion models requires reliable numerical and experimental comparison techniques. In this context, a reverse ray - tracing method was introduced to generate high resolution pseudo - OH images, significantly improving the consistency between CFD predictions and experimental measurements in high pressure rocket combustion applications [17]. Rotary kiln combustion has been extensively studied using CFD due to its relevance in high temperature industrial processes. Investigations of methane fired rotary kilns demonstrated that primary air swirl intensity, annulus diameter, and secondary air temperature have a strong influence on flame length and flow structure. An increase in swirl intensity and annulus diameter was found to result in flame elongation [18]. CFD simulations using ANSYS Fluent have been widely applied to cement and iron - ore pelletizing kilns to analyse combustion and heat transfer characteristics. These studies emphasized the importance of temperature distribution, gas velocity fields, and heat losses. In addition, the applicability of alternative fuels, such as biogas and sewage sludge, for improving kiln performance was successfully demonstrated [19, 20]. Further numerical studies have addressed multi fuel operation in rotary lime kilns using coupled CFD and finite-element methods. Among the fuels considered, Corex gas was selected for detailed investigation owing to its favourable chemical composition and calorific value [21]. The co - combustion of petcoke and olive pomace in cement rotary kiln burners has also been investigated using ANSYS Fluent with different k - ε turbulence and combustion models. The hybrid finite rate, eddy dissipation model was shown to provide more accurate predictions of temperature fields and species concentrations than the conventional k - ε model, while maintaining acceptable computational efficiency [22].

Correlations between flame length and dimensionless heat release rate (HRR) have been established using scaled models and CFD simulations to forecast fire severity under various circumstances [23]. CFD simulations studied axial flow mixing in a tunnel kiln preheating zone, evaluating temperature distribution and differences. Two nozzles on opposite walls improved mixing, especially up to an IFR of ~ 4 N. CFD results agreed with analytical predictions within 0.5 % error [24]. Increasing biomass lowers furnace exit temperature and CO_2 and NO_x emissions, according to CFD research of coal sawdust co firing

in the Paiton power plant. Stable furnace operation is facilitated by ideal sawdust ratios. For effective combustion and emission management, the right fuel mix is essential [25]. Two-way coupled and non-coupled models of an automobile turbine rotor were evaluated using CFD and FSI simulations. Although flow at the tongue and blade structural response varied, overall turbine performance was comparable. Accurate analysis requires detailed flow-structure interactions [26].

CFD is used to study coal reactions such as devolatilization, combustion, and gasification. The research investigates soot formation and compares detailed and soot - included models. Effects of O_2 to CO_2 concentration on soot behaviour during gasification are analysed [27]. Although a free piston engine linear generator (FPELG) has minimal emissions and excellent efficiency, its lack of a crankshaft causes performance problems. Fuel injection duration (FID) has a major impact on the output and behaviour of combustion. Efficiency was increased by achieving optimal performance at FID 14 - 17 ms [28]. Oxidation in air was investigated using thermogravimetric analysis of Loy Yang and Newlands coals. Heat and mass transmission with mass loss from oxidation were simulated numerically. Burn - off time was influenced by coal rank, particle size, and oxygen content [29]. RSM was used to maximize the yield of two biodiesel samples made from cooking oil, beef tallow, and oil. Both were tested in a diesel engine with varying loads and satisfied ASTM D 6751 requirements. Compared to Sample 1, Sample 2 demonstrated reduced fuel consumption and increased brake thermal efficiency [30].

Unfortunately, there is limited information about the characteristics of flames for the annular ring burners with gaseous fuels if the combustion chamber contains a combustion gas. A simplified 2 - D axisymmetric model, which is 20 meters long and has a 10 meters diameter, is used in the simulation of non-premixed diffusion flame for annular ring burner. This study presents the effects of annular ring burner geometrical features and operating circumstances on flame patterns. The models predict the effects of air velocity, access air number, and O_2 - concentration in the combustion gas on the axial temperature profiles and flame behaviour.

Overview of CFD modelling

Computational fluid dynamics applies mathematics, physics, and computational tools to simulate and visualize fluid flow and its interaction with objects. Therefore, CFD is often referred to as the numerical simulation of flow fields. Most CFD analyses are based on the Navier Stoks equations describe the motion of fluids, which define any single - phase fluid flow. And these equations can be simplified by removing terms describing viscous actions to get the Euler equations. There are also some basic methods (finite-volume method and finite-element method) to solve the governing equations of the numerical simulation. For turbulence modelling, the k - ε turbulence model is used. The field variables are calculated using default schemes. CFD can be used in the analysis of the characteristics of combustion flow. Through the analysis of the CFD modelling, temperature contours and velocity vectors can be used to show the combustion zones and the temperature distribution. Moreover, the efficiency of combustion can be provided by analysing the species concentration. CFD modelling works out the consequences of mathematical model, rather than a physical model. All the detail data of combustion can be calculated using computer, these data will make a great difference on the study of combustion. Some parameters of flames that are difficult to measure in the experiment will be clearly presented by CFD modelling. Regarding the ANSYS Fluent solver, the governing equations used in the present CFD simulations including the continuity, momentum, and energy equations are presented by ANSYS [31] and Ciappi et. al. [32].

Non-premixed combustion model

The non-premixed modelling approach is specifically designed to simulate turbulent flames, which involve fast combustion reactions. This approach is widely used in many industries because burners with turbulent non-premixed flames allow for control over the amount of air and can operate with various types of fuel. In the non-premixed model, a key assumption is that the instantaneous thermochemical state of the fluid depends on a conserved scalar called the mixture fraction, denoted by f. The mixture fraction represents the fraction of mass that originates from the fuel stream relative to the total mass of the mixture.

The mixture fraction f can be defined as the ratio of the mass of material originating from the fuel stream to

the total mass of the mixture, as shown in Eq. (1). It can also be expressed in terms of elemental mass fractions as in Eq. (2) [33]:

$$f = \frac{Mass\ of\ Material\ having\ its\ origin\ in\ the\ fuel\ stream}{Mass\ of\ mixture} \quad (1)$$

$$\text{Maxture fraction } (f) = 1 - \frac{Z_{i,ox} - Z_i}{Z_{i,ox} - Z_{i,fuel}} \quad (2)$$

Here, Zi represents the mass fraction of element i. The subscript ox refers to values at the oxidizer inlet, while the subscript fuel corresponds to values at the fuel inlet.

The mass fraction is equal to 1 in the fuel stream and 0 in the oxidizer stream, while within the flow domain it varies continuously between 0 and 1.

Assumptions

The free jet flame simulation will be researched in this study, and the major assumptions are as follows:

- Axis-symmetry model. The offset at the center of the kiln makes flow asymmetric about the kiln axis.
- Steady state. It is assumed that the fluctuation of the fuel and air velocity will have little to no effect on the flame characteristics.
- Buoyancy effect will be neglected. The high primary jet momentum will be operated in kilns and the surrounding combustion gas temperature is also very high. The Richardson number equals to 0.001, this value will prevent buoyancy from having a significant effect on the flame dynamics [34].
- Incompressible flow. The kiln burner works at supersonic flows, Mach number (Ma) = 0.6 [34]. Hence, this allows the flow to be modelled as incompressible.

Geometry and mesh generation

Annular ring burner will be proposed in this research, and this burner will be used in jet flame simulation. The geometry of annular ring burner is shown in Fig. 1. The inner orifice diameter is 50 mm to inject the fuel, and the outer diameter is an alterable diameter for injecting air. In this study, we used Methane as a fuel and injected it with a constant velocity of 30 m s^{-1}. While the annular diameter and excess air number of the combustion gas are changed. To study the effect of annular diameter on flame length we used different annular diameters. Table 1 summarized the boundary conditions of annular ring burner.

Fig. 2 shows the schematic diagram for the non-premixed flame configurations, which used in the

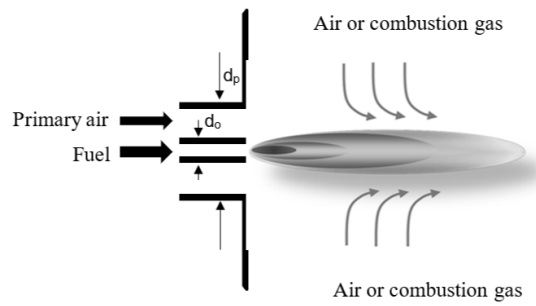

Fig. 1. Annular ring burner with different surrounding gas .

Table 1. Boundary conditions of annular ring burner.

Fuel	Fuel Velocity u_o, $m.s^{-1}$	Air Temperature $T_{air,}$ °C	Volume Flow Rate of gas $v_{comb.}$ gas, $m^3\ s^{-1}$
CH_4	30	20	873 - 1273
	Volume Flow Rate of Air V_o, m^3s^{-1}	Outer Diameter d_o, mm	Outer to the inner Diameter d_p/d_o
	0.0589	50	3.7-31.1

rotary kiln flame simulation. The mesh generated in ANSYS ICEM package which is shown in Fig. 2b. The primary air to fuel inlet diameter ratio is 10.6 (dp/do= 10.6). According to the boundary-layer theory, near the burner end, the mesh is condensed. A velocity inlet is used to define air and Methane, while the outlet is defined as a pressure outlet. As to jet flame simulation, mesh independence study should be the first and most important work, it will contribute to high accurate results in a short time. The properties for simulated fuels (CH_4) are tabulated in Table 2.

In this study, the mesh resolution is varied from 5 000 to 100 000 cells as shown in Fig. 3. This figure demonstrates that the coarse mesh is a large variation of the flame length, while the relative variation became 0.5 % with the grid number of more than 20 000 cells. Therefore, the grade of 30 000 cells is selected to carry out the annular burner simulation.

RESULTS AND DISCUSSION

Case study of air atmosphere combustion chamber

The axial mixture fraction in dimension less and temperature distribution in the axial direction is used to study flame characteristics with change in annular ring burner diameter as shown in Fig. 4, 5, and 6.

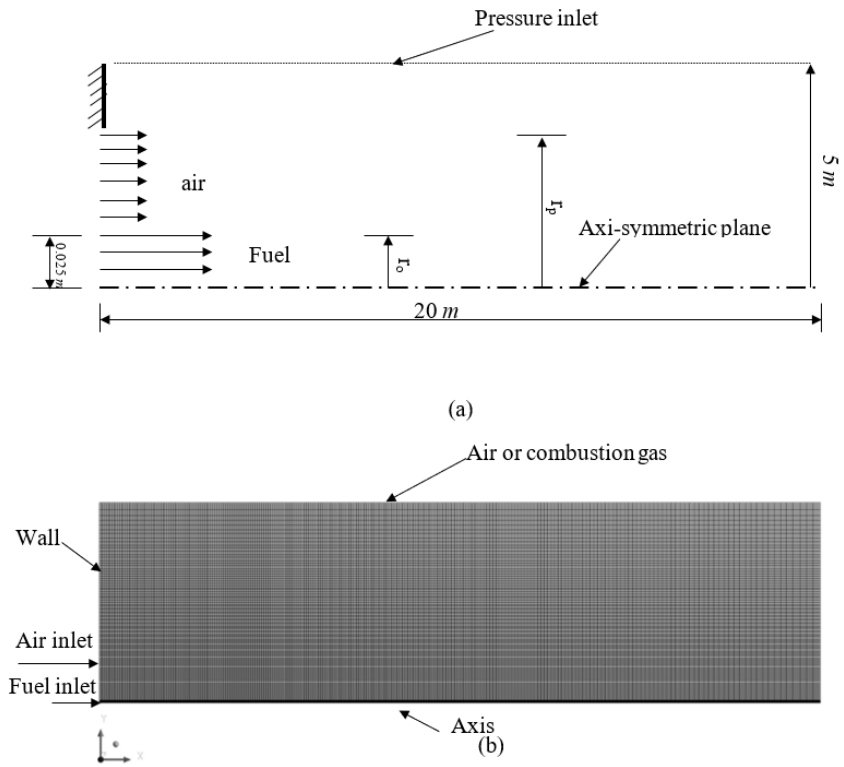

Fig. 2. 2D domain geometry and mesh for free jet flame simulations: (a) geometry, (b) mesh.

Table 2: Physical and thermal properties of CH_4.

Fuel	Air demand L, kg_{air}/kg_o	Fuel Density ρ_o, 20^oC, kg m^{-3}	Heating value hu(net), MJ kg_o^{-1}
CH_4	17.3	0.668	50
Molar Mass Mo, kg $kmol^{-1}$	Volumetric air demand, m^3_{air} M^{-3}_o	Mixing fration, f_{st}	Thermal condictivity K, W. m^{-1} K^{-1}
16	9.52	0.055	0.035

From Fig. 4 can note that the peak temperature near the burner tip then decreases along the flame direction this behaviour with different dp/do values. Where, by increasing the annular diameter, the peak temperature changed from 1600℃ to above 2000℃ also can note that the highest temperature point shifted to the right by more than 200 %. This phenomenon is attributed to an increase in the area between air and fuel by increasing the annular diameter and that leads to making the flame long. It can also be noted that the

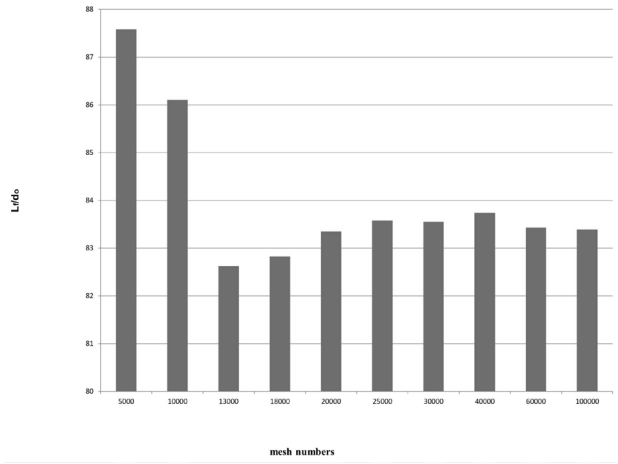

Fig. 3. Mesh independence study for free jet dimensionless flame length.

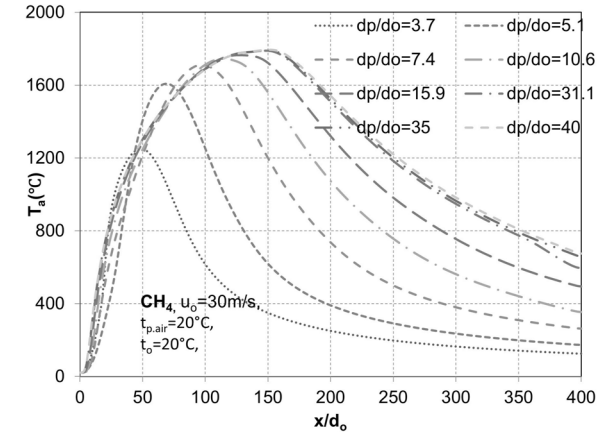

Fig. 4. Influence of annulus diameter on axial temperature distribution along the flame.

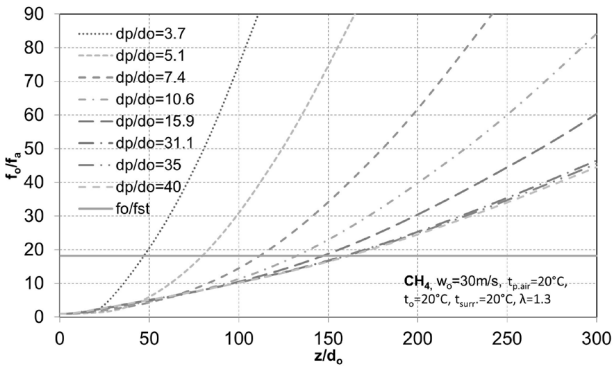

Fig. 5. Influence of annulus diameter on inverted dimensionless axial mixture fraction profiles along the flame.

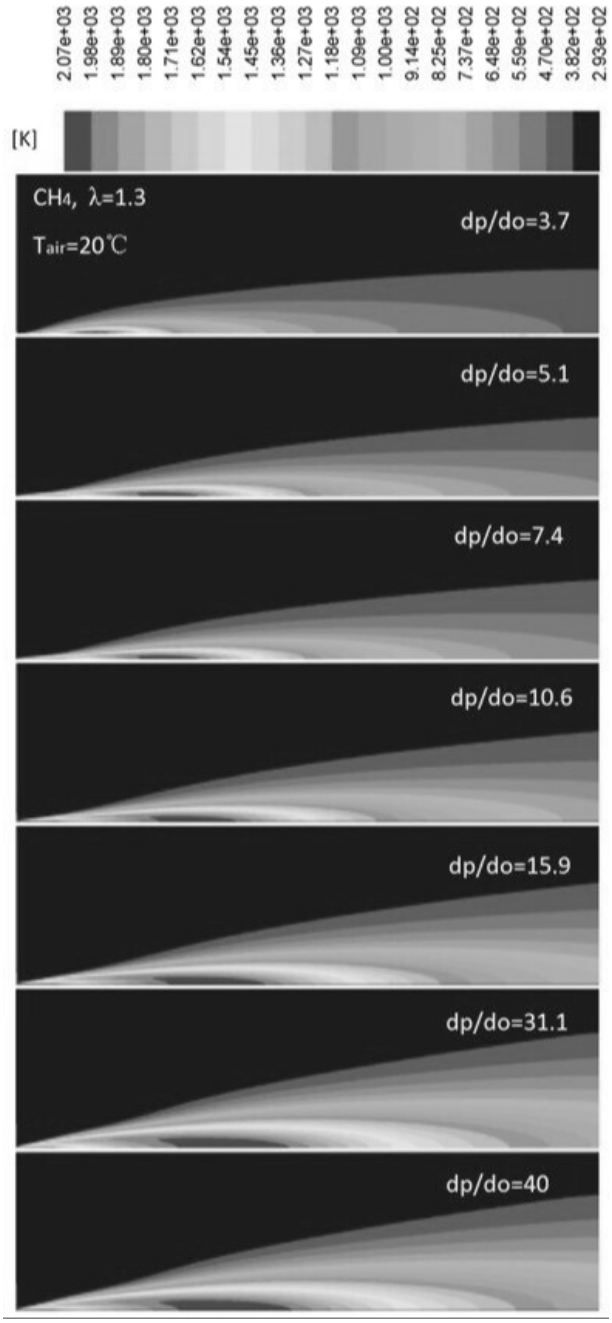

Fig. 6. Influence of annulus diameter on temperature contours.

peak temperature points decreased to when the annulus diameter is decreased because the high air velocity with a smaller annular diameter enhances the mixing of air and fuel, because that the combustion process occurs within a relatively short length. The peak and position of temperature do not change anymore after the diameter ratio 31.1, consequently, the flame length is not increased.

The dimensionless mixture fraction along the flame as a function of annular diameter is shown in Fig. 6. Here, the measurement of flame length is based on the conserved scalar mean mixture fraction. The flame length is measured up to the point where the simulated mean mixture fraction equals the stoichiometric value.

From Fig. 5, it can be observed that the annular diameter has a great influence on flame length, whereby increasing dp/do from 3.7 to 31.1 the flame length is increased from 50 to more than 150 while after dp/do more than 31.1 the flame length will not change any more. Consequently, both flame temperature and flame length will be invariable from Fig. 4 and Fig. 5. In addition, the results of the Fig. 5 also shows that a smaller annulus diameter results in a shorter the flame. And this can be explained by the mixing process will affect the combustion process. A higher air velocity from a smaller annulus diameter that will leads to a better mixing in a short distance, which will lead to a short flame length.

Fig. 6 shows the contours of temperature along the flame with different annular diameters. From these Figure, we can note that increasing air inlet diameter the peak temperature increases and shifts to the right. This result is same with the Fig. 4. As it explained in Fig. 4, the smaller the annulus diameter, the better the mixing process, the combustion process will complete over a shorter length. This is the reason why the peak temperature point shifts to right.

Case study of air atmosphere combustion

Ambient environment will make a great difference on the simulation result. When the ambient is combustion gas, the excess air number will affect the result directly, and the stoichiometric mixture fraction is used to definite the flame length. It can be predicted that the flame length will be longer with a relatively large excess air number of primary air and the peak temperature is also become larger. However, the definition of flame length is also changed. The equilibrium method has been used to calculate the flame length.

The impact of the excess air number on the axial temperature distribution is depicted in Fig. 7. Along the flame axis, the temperature always rises at first before falling. There is little difference in the temperature profiles' overall shape near the burner rim. The peak flame temperature shows a distinct trend as the excess air number is decreased; it falls. The greatest and lowest surplus air number situations exhibit peak temperatures that differ by about 100°C, underscoring the important influence of the air-fuel ratio on combustion intensity.

The flame length as a function of excess air number $\lambda_{comb.gas}$ is shown in Fig. 8. From this figure note that increasing excess air number decreases flame length with a slightly affect. Moreover, this influence decreases with the increase of the excess air number. It can be predicted that with $\lambda_{comb.gas} \geq 10$ the flame length does not change.

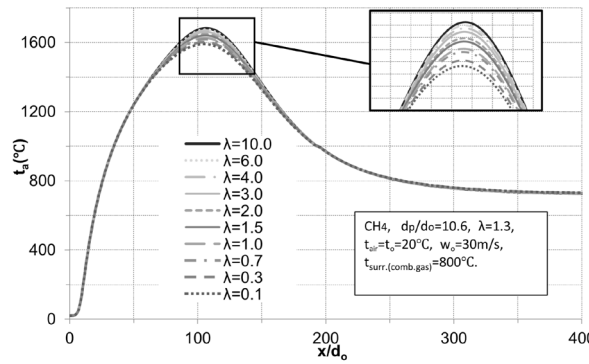

Fig. 7. Influence of excess air number of the combustion gas on axial temperature profiles along the flame.

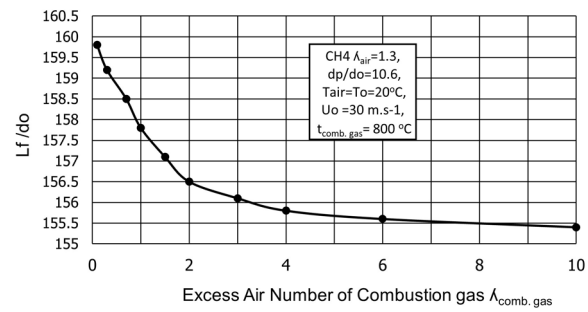

Fig. 8. Influence of excess air number of combustion gas on dimensionless flame length.

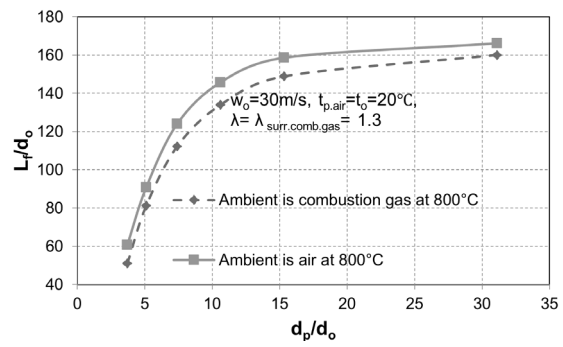

Fig. 9. Dimensionless flame length as a function of dimensionless annular diameter at the surroundings is air and combustion gas.

Fig. 9 shows the comparison of non-dimensional flame length with different annulus diameters using different ambients. It can be noted that the non-dimensional flame length increased with increased annular diameter.

In addition, the ambient gas causes a small change in flame length. In general, the flame length in case of ambient is combustion gas, it is longer than in case the ambient is air.

It can be explained that the O_2 - concentration of air surroundings is higher than the combustion gas surroundings, and the higher the concentration of O_2 the better the mixing between fuel and O_2 that leads to the combustion process complete in a short distance (short flame length). The maximum difference of flame length between air surroundings and combustion gas surroundings is ~ 4 %.

CONCLUSIONS

The simulation of non-premixed flames is separated into two sections: combustion gas and air borne methane flames. The air-based simulation is a first step toward a more realistic analysis because actual burners work in combustion gas fields.

In case the surrounding medium is air, the results show that

- The annular diameter significantly influences the temperature and length of flame.
- The maximum temperature increases and the position of peak temperature is located away from the annular orifice when the annulus diameter is increased.
- Increasing the annular diameter lead to increase the flame length.

When the ambient is combustion gas

- Increasing the annular diameter lead to increase the flame length.
- The flame length has a small effect by the excess air number of combustion gas.

Acknowledgments

I would like to express their heartfelt thanks to Prof. E. Specht, Magdeburg University, Magdeburg, Germany for his valuable guidance, continuous support, and encouragement throughout the research work. Also I would to thanks the staff of Electromechanics Eng. University of Technology Baghdad for their assistance.

Authors' contributions

A.G.T. Al-H.: Conceptualization, methodology, data analysis, writing - original draft, data collection, writing; E. S.: Supervision, review, funding.

REFERENCES

1. M. Peter, J. Barrie, Flames and Burners for Furnaces, Industrial and Process Furnaces, 2nd Edition, 2013.
2. C.E. Baukal, Industrial burners handbook, CRC Press LLC, 2004.
3. C.E. Baukal, The John Zink combustion handbook, CRC Press, LLC, 2001.
4. C.E. Baukal, Industrial combustion pollution and control, Marcel Dekker, Inc., 2004.
5. K. Vít, B. Petr, O. Jaroslav, S. Petr, Testing of gas and liquid fuel burners for power and process industries, Energy, 33, 2008, 1551-1561.
6. H.F. Elattar, R. Stanev, E. Specht, A. Fouda, CFD simulation of confined non-premixed jet flames in rotary kilns for gaseous fuels, Computers & Fluids, 102, 2014, 62-73.
7. H.F. Elattar, Flame simulation in rotary kilns using computational fluid dynamics, Ph.D. dissertation, Germany, Magdeburg University, 2011.
8. A. García, M.A. Rendon, A.A. Amel, Combustion model evaluation in a CFD simulation of a radiant-tube burner, 276, 2020, 118013.

9. N.B. Arkhazloo, Y. Bouissa, F.B.Tehrani, M. Jadidi, J. Morin, M. Jahazi, Experimental and unsteady CFD analyses of the heating process of large size forgings in a gas-fired furnace, J. Cas studies in thermal engineering, 14, 2019, 100428.
10. L. Pachec, F. López, J. Saldaña, J. Trinidad, M. Pérez, W. Ángel, R. León, Design and numerical analysis of an annular combustion chamber. J. Fluids, 9, 2024, 161.
11. A.G.T. Al-Hasnawi, E. Specht, A compartive analysis of different special injection burner design by using CFD, J. Chem. Technol. Metall., 52, 1, 2017, 137-147.
12. F. Tonti, J. Perovšek, J.Z. Usandivaras, S. Karl, J.S. Hardi, Y. Morii, M. Oschwald, Obtaining pseudo - OH radiation images from CFD solutions of transcritical flames, Combustion and Flame, 233, 2021, 111614.
13. J. Arroyo, C. Pillajo, J. Barrio, P. Compais, D. Tavares, Deep learning techniques for enhanced flame monitoring in cement rotary kilns using petcoke and refuse-derived fuel (RDF), Sustainability, 16, 2024, 6862.
14. A.S. Singh, Y. Vijrumbana, V. Mahendra, Experimental and computational (Chemical Kinetic + CFD) analyses of Self-Recuperative annular tubular porous burner for NH_3/CH_4 - air Non -Premixed combustion, J. Chemical Engineering, 481, 2024, 148439.
15. D.M. Cecílio, M. Mateus,A.I. Ferreiro, Industrial rotary kiln burner performance with 3D CFD modeling, MDPI, Fuels, 4, 2023, 454-468.
16. M. Li, Z. Wang, J. Jiang, W. Lin, L. Ni, Y. Pan, G. Wang, Numerical simulation and consequence analysis of full-scale jet fires for pipelines transporting pure hydrogen or hydrogen blended with natural gas, MDPI, J. Fire, 7, 2024, 180.
17. A.A. Moreno, M. Ángel, C. Lascorz, V. Tavares, An industrial - scale cement rotary kiln CFD model to characterise altenative fuel combustion profiles, the 36^{TH} inernational conference on efficiency, cost, optimization, simulation, and environmental impact of energy systems, Spain, 2023, 448-459.
18. H.F. Elattar, E. Specht, A. Fouda, S. Rubaiee, A. Al - Zahrani, S.A. Nada, Swirled jet flame simulation and flow visualization inside rotary kiln - CFD with PDF approach, MDPI, Processes, 8, 2020, 159.
19. H. Alfredo, A.P. Hernandez, J. Morales-castillo, CFD model for the simulation of the combustion of alternative fuels in a rotary kiln, J. Revista International, 9, 2021, 53.
20. I.A. Larsson, A.L. Ljung, D. Marjavaara, Simulation of thermal effects on the flow field in a pilot-scale kiln mining, Metallurgy & Exploration, 38, 2021, 1487-1495.
21. D. Kumar, A.K. Dewangan, Computational fluid dynamics modelling of the rotary lime kiln, Heat and mass transfer conference, India, 2021, 6573.
22. Z. Ngadip, M.L. Lahlaouti, CFD modeling of petcoke co - combustion in a real cement kiln: The effect of the turbulence-chemistry interaction model applied with K - ε variations, International Review of Applied Sciences and Engineering, 13, 2022, 148-163.
23. R. Xu, C. Tao, K. Wang, P. He, Q. Wu, W. Zhao, The investigation of flame length and flow field structure in the underground vertical channel with different opening areas, Tunnelling and underground space technology incorporating trenchless technology research, 111, 2021, 103846.
24. A.G.T. Al-Hasnawi, H.A. Refaey, T. Redemann, M. Attala, E. Specht, Computational fluid dynamics simulation of flow mixing in tunnel kilns by air side injection, Journal of Thermal Science and Engineering Applications, 10, 2018, 031007.
25. Ch. Chairunnisa, M.P. Helios, A. Andini, A.P. Nuryadi, A. Maswan, H. Sutriyanto, H. Pujowidodo, B.T. Prasetyo, A.D. Nugraha, N. Cahyo, Numerical modelling Co - firing combustion in the existing coal-fired power plant: case study in paiton 9 power plant, EVERGREEN Joint Journal of Novel Carbon Resource Sciences and Green Asia Strategy, 11, 03, 2024, 2638-2649.
26. N.Z.A. Bakar, M.H. Padzillah, Comparison between computational fluid dynamics and fluid-structure interaction Models of an automotive mixed flow turbocharger turbine, EVERGREEN Joint Journal of Novel Carbon Resource Sciences and Green Asia Strategy, 11, 2, 2024, 1457-1470.
27. A.T. Wijayanta, A.M. Saiful, K. Nakaso, J. Fukai, Detailed reaction mechanisms of coal volatile combustion: comparison between without soot and soot models, Journal of Novel Carbon Resource Sciences, 2, 2010, 8-11.
28. A. Raheem, A.R.A. Aziz, S.A. Zulkifli, A.T. Rahem, W.B. Ayandotun, S.M. Elfakki, M. Baharom, E.Z.

Zainal, Combustion characteristics of a free piston engine linear generator using various fuel injection durations, EVERGREEN Joint Journal of Novel Carbon Resource Sciences & Green Asia Strategy, 10, 01, 2023, 594-600.
29. S. Nozawa, N. Wada, Y. Matsushita, T. Yamamoto, M. Omori, T. Harada, Experimental and numerical investigation of effect of coal rank on burn -off time in pulverized coal combustion, EVERGREEN Joint Journal of Novel Carbon Resource Sciences, 5, 2012, 23-27.
30. B.J. Venkatash, V.M. Kulkarni, K.N. Krishnamurthy, K.M. Vinay, Optimizing biodiesel yield and investigating CI engine performance using biodiesel blends of pongamia, animal fat, and waste cooking oils, EVERGREEN Joint Journal of Novel Carbon Resource Sciences & Green Asia Strategy, 11, 3, 2024, 1808-1819.
31. ANSYS Inc., ANSYS FlUENT 14.0, Theory Guide, Canonsburg, USA, 2009.
32. L. Ciappi, M. Stebel, J. Smolka, L. Cappietti, G. Manfrida, Analytical and computational fluid dynamics models of wells turbines for oscillating water column systems, J. Energy Resour Technol., 2022, 144.
33. E. Specht, Lecture Notes of combustion engineering, University of Magdeburg, Germany, 2014.
34. A.H. Alyaser, Fluid flow and combustion in rotary kilns, Ph.D. dissertation, The University of Britisch Columbia, Vancouver, Canada, 1998.